






**Fully differential investigation of two-center interference in dissociative capture in  $p + \text{H}_2$  collisions**S. Bastola <sup>1</sup>, M. Dhital <sup>1,\*</sup>, B. Lamichhane<sup>1,†</sup>, A. Silvus <sup>1,‡</sup>, R. Lomsadze <sup>2</sup>, J. Davis<sup>1</sup>, A. Hasan<sup>3</sup>,  
A. Igarashi<sup>4</sup> and M. Schulz <sup>1,§</sup><sup>1</sup>Physics Dept. and LAMOR, Missouri University of Science & Technology, Rolla, Missouri 65409, USA<sup>2</sup>Dept. of Exact and Natural Science, Tbilisi State University, Tbilisi 0179, Georgia<sup>3</sup>Dept. of Physics, UAE University, P.O. Box 15551, Al Ain, Abu Dhabi, UAE<sup>4</sup>Faculty of Engineering, University of Miyazaki, Miyazaki 889-2192, Japan

(Received 3 December 2021; accepted 25 February 2022; published 11 March 2022)

We have measured and calculated fully differential cross sections for vibrational dissociation following capture in 75-keV  $p + \text{H}_2$  collisions. For a molecular orientation perpendicular to the projectile beam axis and parallel to the transverse momentum transfer we observe a pronounced interference structure. The positions of the interference extrema suggest that the interference term is afflicted with a phase shift which depends on the projectile scattering angle. However, no significant dependence on the kinetic-energy release was observed. Considerable discrepancies between our calculations and experimental data were found.

DOI: [10.1103/PhysRevA.105.032805](https://doi.org/10.1103/PhysRevA.105.032805)**I. INTRODUCTION**

Already more than six decades ago Tuan and Gerjuoy predicted two-center interference effects in electron capture in  $p + \text{H}_2$  collisions [1]. Since as a matter of principle it is not possible to distinguish from which atomic center of the molecule the projectile is diffracted, the transition amplitudes for both possibilities have to be added coherently. This can lead to interference structures in the cross sections as a function of parameters which determine the phase angle in the interference term. It took another three decades before such interference structures were experimentally identified in cross sections differential in the molecular alignment for dissociative capture in  $\text{O}^{8+} + D_2$  collisions [2]. Later, they were also found in double-differential spectra of electrons ejected from  $\text{H}_2$  by highly charged ion impact [3]. These studies sparked major activities on experiments studying such interference effects in more detail (e.g., Refs. [4–10]).

Perhaps the most detailed study of such interference effects was performed in a kinematically complete experiment on 10-keV  $\text{H}_2^+ + \text{He}$  collisions [5]. There, electron transfer from the target to the dissociative  $2p\sigma_u$  state of the projectile was selected. For fixed molecular orientation and kinetic-energy release (KER) the fully differential cross sections (FDCS) were presented as a function of the recoil-ion momentum. Very pronounced interference structures were observed. However, the patterns were afflicted with a phase shift of  $\pi$  relative to the expected theoretical two-center interference term  $I_2$

[11]. This was convincingly explained by parity conservation: the switch of symmetry of the molecular state from gerade to ungerade during the transition must be compensated by a corresponding switch in symmetry of the He atom in its motion relative to the molecular projectile.

The same  $\pi$ -phase shift was also observed in FDCS for target ionization accompanied by projectile excitation to the  $2p\sigma_u$  state in 1-MeV  $\text{H}_2^+ + \text{He}$  collisions, which involves the same symmetry switch of the molecular state [9]. On the other hand, no phase shift was found in the cross sections for electron capture accompanied by electronic excitation to a dissociative state of the residual molecular ion in 1.3-MeV  $p + \text{H}_2$  collisions [6]. Although this experiment was not strictly state selective, the selected KER range of 5 to 8 eV should have strongly favored dissociation through the  $2p\pi_u$  state. Based on the reasoning of Ref. [5] a  $\pi$ -phase shift was to be expected in the data of Ref. [6] as well. To the best of our knowledge this apparent conflict has not been resolved yet. We do point out, however, that our data for the same process as studied in Ref. [6], but for a projectile energy of 75 keV and a KER range of 5 to 12 eV [12], are consistent with the explanation offered in Ref. [5].

Another dissociation channel in which a phase shift was observed in the interference pattern is known as ground state [13] or vibrational dissociation [10]. There, the dissociation is not caused by an electronic transition to a dissociative state, but rather by an excitation of the nuclear motion to a vibrational continuum state. Disregarding the vibrational state, the molecular ion ( $\text{H}_2^+$ ) remains in the ground state. A  $\pi$ -phase shift was observed in the FDCS for vibrational dissociation following target ionization in 200-eV  $e^- + \text{H}_2$  [13] as well as for vibrational dissociation following electron capture in 75-keV  $p + \text{H}_2$  collisions [10]. What is remarkable about these findings is that in these dissociation channels the electronic transition does not lead to a switch in the symmetry of the molecular state. Therefore, the explanation for the

\*Present address: Physics Dept., University of California-Riverside, Riverside, CA 92521.

†Present address: Earlham College, Richmond, IN 47374.

‡Present address: Department of Radiation Oncology, Washington University, St. Louis, MO 63110.

§schulz@mst.edu

phase shift based on parity conservation, which is plausible for dissociation through electronic excitation to an ungerade state, may not hold to explain the observations for vibrational dissociation. However, it has been pointed out that the explanation based on parity conservation cannot be entirely ruled out because apart from the symmetry of the electronic molecular state the one of the state of the nuclear motion (i.e., vibrational and rotational) also needs to be considered [14]. On the other hand, it is not clear why antisymmetric nuclear states would be favored by the collision process.

The data on dissociative capture in  $p + \text{H}_2$  collisions were compared to calculations based on two different models. The first one [10,15] represents an *ad hoc* approach in two regards: first,  $I_2$  is not calculated from first principles, but rather the cross sections for the incoherent case are multiplied by the model interference term reported in Ref. [11]. Second, a phase shift of  $\pi$  was introduced to match the calculated interference pattern with the one observed in experiment. In contrast, the second model [16,17] does not make any assumptions about a  $\pi$ -phase shift. In the calculations of the cross sections as a function of  $\theta_p$ , the position of the interference extrema at small  $\theta_p$  is consistent with a phase shift of 0 relative to  $I_2$  from Ref. [11]. There, the calculation is not in good agreement with the experimental data. However, at larger  $\theta_p$  the position of the interference extrema seemed to depart from what is expected for a zero-phase shift and somewhat better agreement with both the experimental data and the calculation based on the first model, assuming a  $\pi$ -phase shift, was obtained. This suggests that in the second model the two-center interference term is more complex than the one reported in Ref. [11]. Parameters which determine the total phase appear to depend on  $\theta_p$ . Furthermore, the calculations were performed for fixed values of KER and the results show that the position of the interference extrema depends on that parameter as well.

In our previous experiment reported in Ref. [10] vibrational dissociation was selected by setting a condition on the KER range 0 to 2 eV. However, we neither had sufficient resolution nor statistics to analyze cross sections differential in KER with a narrow bin size. In this paper we report FDGS for fixed KER as a function of  $\theta_p$ . This was achieved by increasing the number of true vibrational dissociation events by more than an order of magnitude and the momentum resolution of the detected fragments by a factor of 5. The results confirm a significant phase shift compared to the interference term reported in Ref. [11]. Furthermore, the phase shift appears to depend on  $\theta_p$ . However, a dependence on KER could not conclusively be identified.

## II. EXPERIMENT

The experiment was performed at the medium energy accelerator of the Missouri University of Science & Technology. A proton beam was generated with a hot cathode ion source and accelerated to an energy of 75 keV. The beam was collimated to a size of  $0.15 \times 0.15 \text{ mm}^2$  by a pair of slits placed at a distance of 50 cm from the target chamber. This slit geometry corresponds to a transverse coherence length of about 3.3 a.u. [18]. In the target chamber, the projectile beam was crossed with a very cold ( $T \cong 1\text{--}2 \text{ K}$ )  $\text{H}_2$  beam generated with a supersonic gas jet. After the collision the projectiles were

charge-state analyzed using a switching magnet. The neutralized beam component was detected by a two-dimensional position-sensitive microchannel plate detector (MCP). From the position information the azimuthal and polar projectile scattering angles were determined with a resolution of  $3^\circ$  and 0.15 mrad full width at half maximum (FWHM), respectively.

The proton fragments from the dissociated target molecule were extracted by a weak electric field of about 7.8 V/cm and traversed a field-free region twice as long as the extraction region in order to achieve optimized time focusing [19]. The fragments were detected by a second two-dimensional position-sensitive MCP detector, which was set in coincidence with the projectile detector. The directions of the extraction field ( $x$  direction) and of the expansion of the target gas ( $y$  direction) define the coordinate system in which the projectile and recoil-ion momenta are analyzed. From the position information, the two momentum components perpendicular to the extraction field (i.e., the  $y$ - and  $z$  components, where the latter coincides with the projectile beam direction) were determined. The  $x$  component of the fragment's momentum  $\mathbf{p}_{\text{fr}}$  was obtained from the time of flight from the collision region to the detector, which, in turn, is contained in the coincidence time. From the momentum components the KER and the molecular orientation were calculated.

Compared to our previous experiment [10], the fragment's momentum resolution was significantly improved by two modifications, one in the experimental setup and one in the data analysis: in the experiment the extraction voltage was reduced from 500 to 100 V. In the data analysis, events with a molecular orientation along the  $x$  axis were selected. Because the target temperature is negligible in this direction, and due to time focusing, the momentum resolution for the  $x$  component is significantly better than for the  $y$  component and somewhat better than for the  $z$  component. Under these circumstances, the momentum resolution comes mainly from the finite size of the interaction volume, i.e., the overlap volume between the projectile and target beams, and the time resolution. It is linearly proportional to the extraction voltage. The corresponding resolution in KER depends on the KER itself and ranges from 30-meV FWHM at  $\text{KER} = 0.2 \text{ eV}$  to 70-meV FWHM at  $\text{KER} = 1.6 \text{ eV}$ . The resolution in the polar and azimuthal angles of the molecular orientation is estimated as  $4^\circ$  and  $8^\circ$  FWHM, respectively. The azimuthal resolution is worse because  $\varphi_{\text{fr}}$  depends on the  $y$  component of  $\mathbf{p}_{\text{fr}}$  (i.e., the component with the worst resolution), while  $\theta_{\text{fr}}$  does not.

## III. DATA ANALYSIS

Immediately after the collision, the  $\text{H}_2^+$  ion moves with a momentum  $\mathbf{p}_{\text{rec}} = \mathbf{q}$ , where  $\mathbf{q}$  is defined as the difference between the initial momentum of the incident proton and the momentum of the scattered neutralized projectile.  $\mathbf{q}$  is related to the momentum transfer from the projectile to the target  $\mathbf{q}'$  by  $\mathbf{q} = \mathbf{q}' - \mathbf{v}_p$ . Here, the transverse component  $\mathbf{q}'_{\text{tr}} = \mathbf{q}_{\text{tr}}$  has magnitude  $q_{\text{tr}} = mv_p \tan \theta_p$  and the longitudinal component of  $\mathbf{q}$  is given by  $q_z = (E_f - E_i)/v'_p - v_p/2$ , where  $m$  and  $\mathbf{v}_p$  are the mass and velocity of the incident proton, respectively.  $E_f$  is the sum of the internal energies of the neutralized projectile and the residual molecular target ion  $\text{H}_2^+$  and  $E_i$  is the internal energy of the initial target  $\text{H}_2$ . The recoil momentum  $\mathbf{p}_{\text{rec}}$  is

equally shared by the two atomic centers of the molecule. The dissociation adds a momentum  $\mathbf{p}_d$  and  $-\mathbf{p}_d$ , respectively, to the fragments, measured relative to the center of mass of the molecular ion. As a result, the detected fragment will have a momentum of  $\mathbf{p}_{fr} = \mathbf{q}/2 + \mathbf{p}_d$  in the laboratory frame. The molecular orientation of  $\text{H}_2^+$  is given by the direction of  $\mathbf{p}_d$ . Therefore, we subtracted  $\mathbf{q}/2$  from the measured momentum  $\mathbf{p}_{fr}$  of the charged molecular fragment to obtain the molecular orientation. Since both transverse momentum components of the projectiles are directly measured (using the position information) and the longitudinal component is known from the energy balance, both the magnitude and the direction of  $\mathbf{q}$  are known. The magnitude of  $\mathbf{q}/2$  ranges from 0.5 a.u. at  $\theta_p = 0.1$  mrad to 8 a.u. at  $\theta_p = 5$  mrad, while  $p_d = 8$  a.u. for  $\text{KER} = 1$  eV. Therefore, this correction for  $\mathbf{q}/2$ , which was neglected in our previous experiment reported in Ref. [10], is negligible at small, but quite important at large  $\theta_p$ .

FDCS were analyzed for two molecular orientations. Both of them are perpendicular to the initial projectile beam direction (i.e.,  $\theta_{mol} = 90^\circ \pm 10^\circ$ ). One is also perpendicular to the transverse momentum transfer  $\mathbf{q}_{tr}$ , while the second is parallel to  $\mathbf{q}_{tr}$  and we refer to them as the perpendicular and parallel orientations, respectively. As mentioned in the previous section, in both cases molecular orientations along the  $x$  axis (within  $\pm 10^\circ$ ) were selected. Therefore, the perpendicular orientation is realized by setting a condition on the azimuthal projectile angle  $\varphi_p = 90 \pm 10^\circ$  (i.e., scattering in the  $y$  direction) and the parallel orientation by setting a condition on  $\varphi_p = 0^\circ \pm 10^\circ$  (i.e., scattering in the  $x$  direction).

For the parallel orientation FDCS were obtained for fixed KERs of 0.2, 0.6, 1.0, and 1.6 eV and plotted as a function of  $\theta_p$ . Furthermore, data integrated from  $\text{KER} = 0$  to 2 eV were analyzed for both orientations and compared to the previously published data [10] which neglected the correction for  $\mathbf{q}/2$  as well as to theory.

#### IV. RESULTS AND DISCUSSION

In Fig. 1 we show the measured cross sections integrated over  $\text{KER} = 0$  to 2 eV for the perpendicular (open symbols) and parallel orientations (closed symbols). For the perpendicular orientation no structure can be discerned, but rather the cross sections just drop off monotonically with increasing  $\theta_p$ . This is the expected behavior because in the two-center interference term

$$I_2 = 1 + \cos(\mathbf{p}_{rec} \cdot \mathbf{D} - \delta) = 1 + \cos(\mathbf{q}_{tr} \cdot \mathbf{D} - \delta), \quad (1)$$

the dot product  $\mathbf{q}_{tr} \cdot \mathbf{D}$  is constant at zero for this orientation.  $\delta$  is a phase shift, which is zero in the original version [11] and yet to be determined for the present case. In contrast, the data for the parallel orientation exhibit a pronounced oscillating pattern with minima at 1.7, 3.8, and 5.7 mrad and maxima at 2.2, 4.5, and 6.8 mrad reflecting the  $\theta_p$  dependence of  $\mathbf{q}_{tr} \cdot \mathbf{D} - \delta$ . Note, however, that the oscillating structure is superimposed on very steeply decreasing cross sections, which introduces some uncertainty to the exact location of the interference extrema.

In Fig. 2 the data for the parallel orientation of Fig. 1 are replotted, but this time in comparison with the corresponding

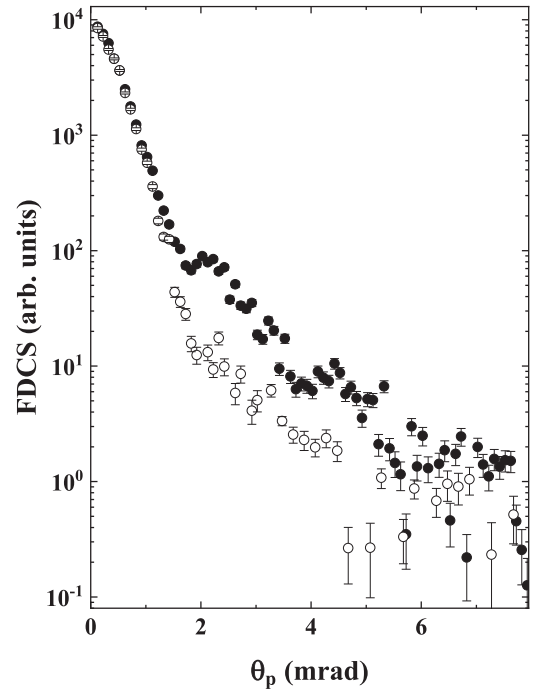


FIG. 1. Fully differential cross sections for all KER and for molecular orientations perpendicular to the initial projectile beam axis and perpendicular (open symbols) and parallel (closed symbols) to the transverse momentum transfer as a function of projectile scattering angle.

data from Ref. [10] shown as open symbols, which we refer to as the old data. To put this comparison in proper perspective, it should be noted that apart from the  $\mathbf{q}/2$  correction another important difference between both data sets lies in the method in extracting the information about the interference pattern. In the new data, it is obtained from a comparison between the coherent FDCS for the parallel and perpendicular orientations (Fig. 1), while in the old data it is obtained from a comparison between the coherent and incoherent FDCS for the parallel orientation. For  $\theta_p$  up to about 1.2 mrad no differences between the two data sets can be discerned, but at larger  $\theta_p$  the correction for  $\mathbf{q}/2$  leads to some differences. The main effect of this correction is that the interference structure becomes more pronounced at large  $\theta_p$ . In fact, in the cross sections of the old data the interference extrema are not fully resolved and only appear as “bumps” in the  $\theta_p$  dependence. Only in the ratios  $R_{||}$  between the cross sections for coherent and incoherent projectiles a clear oscillating pattern was observed. The positions of the interference extrema in these ratios are generally shifted to slightly smaller  $\theta_p$  compared to those seen in the cross sections of the present data.

The  $R_{||}$  for the old data were fairly flat up to about  $\theta_p = 0.8$  mrad. This ratio was thought to represent a product of the interference terms for two-center molecular and single-center interference  $I_1$  [20]. The latter was obtained from the coherent and incoherent cross sections for the perpendicular plane, for which  $I_2$  was assumed to be constant.  $I_2$  was then extracted as a double ratio between  $R_{||}$  and  $I_1$ . It showed a pronounced minimum at  $\theta_p = 0$ , which was taken as a first hint that  $I_2$  is afflicted with a  $\pi$ -phase shift. This analysis has to be

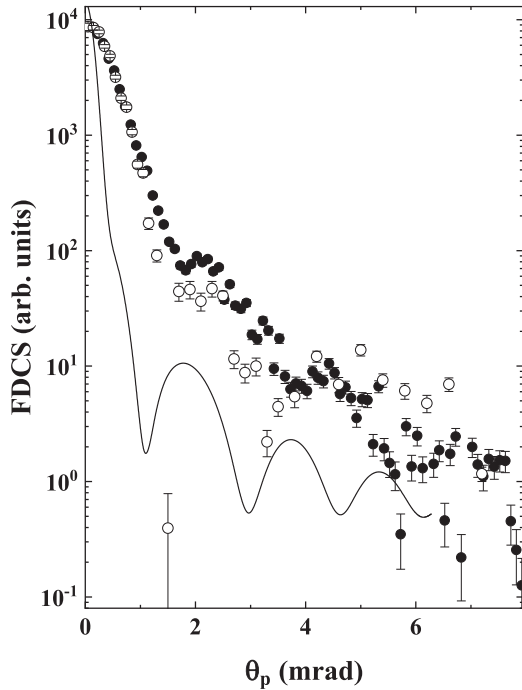


FIG. 2. The data of Fig. 1 for the parallel orientation replotted in comparison to the data of Lamichhane *et al.* [10]. The solid curve shows our calculation.

reconsidered based on the present data. In the new experiment, one important objective was to optimize the recoil-ion momentum resolution. This precluded measuring the cross sections for coherent and incoherent projectile beams simultaneously, as was done in Ref. [10]. This would require obtaining either the coherent or the incoherent data for molecular fragments ejected in the  $y$  direction, for which the recoil momentum resolution is significantly worse than for the  $x$  direction. On the other hand, it should be possible to isolate  $I_2$  as a ratio between the coherent cross sections for the parallel and perpendicular orientations under the assumption that the incoherent part of the cross section is independent of the molecular orientation. However, Fig. 1 strongly suggests that this assumption is not justified for  $\theta_p$  larger than about 1.5 mrad, where the data for the perpendicular orientation are systematically smaller than for the parallel orientation by a large factor. The assumption may be valid for smaller  $\theta_p$ , where the two data sets nearly coincide. If it is, then the similarity between the cross sections for both orientations in this region suggests that here, interference effects are weak.

Since no interference pattern is discernible for small  $\theta_p$ , the behavior at  $\theta_p = 0$  obviously cannot be used to make any conclusions about the phase shift  $\delta$  in  $I_2$ . In the following, we therefore attempt to gain that information from the location of the interference extrema observed for  $\theta_p > 1$  mrad. According to Eq. (1) the extrema occur when  $\mathbf{q} \cdot \mathbf{D} - \delta = n\pi$ , which for the parallel orientation becomes  $mv_p \tan \theta_p D - \delta = n\pi$ . This relation is not sufficient to determine both  $D$  and  $\delta$  at the same time. We therefore first determine an average value of  $D$  under the assumption that  $\delta$  is either 0 or  $\pi$  as a function of  $\theta_p$ . These data are shown in Fig. 3 as open ( $\delta = 0$ ) and closed symbols ( $\delta = \pi$ ), respectively. The horizontal dashed

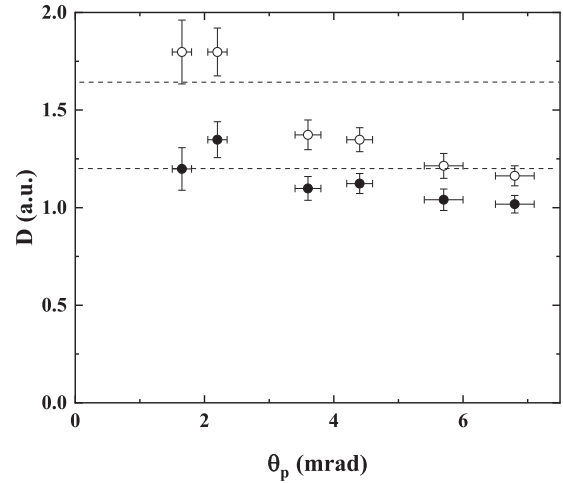


FIG. 3. Internuclear distance  $D$  of the molecule at the instant of the transition extracted from the location of the interference extrema under the assumption that there is no phase shift in the interference term (open symbols) or a phase shift of  $\pi$  (closed symbols).

lines indicate the location of the classical inner and outer turning points for the ground-state vibration of  $\text{H}_2$ . At small  $\theta_p$  the data favor  $\delta = \pi$  as the assumption  $\delta = 0$  results in  $D$  larger than the location of the outer turning point. Likewise, at large  $\theta_p$  the assumption  $\delta = \pi$  results in  $D$  smaller than the location of the inner turning point. A value of  $D$  close to the inner turning point is consistently obtained if  $\delta$  is assumed to evolve from around  $\pi$  at  $\theta_p = 1.5$  mrad to around 0 for  $\theta_p > 5$  mrad. Such a dependence of  $\delta$  on  $\theta_p$  is indeed found if  $\delta$  is calculated under the assumption  $D = 1.2$  a.u., the location of the inner turning point [21], which is plotted in Fig. 4. Indeed, vibrational dissociation is expected to strongly favor the inner turning point [22] because of the maximized overlap between the nuclear wave functions for the initial and final vibrational states.

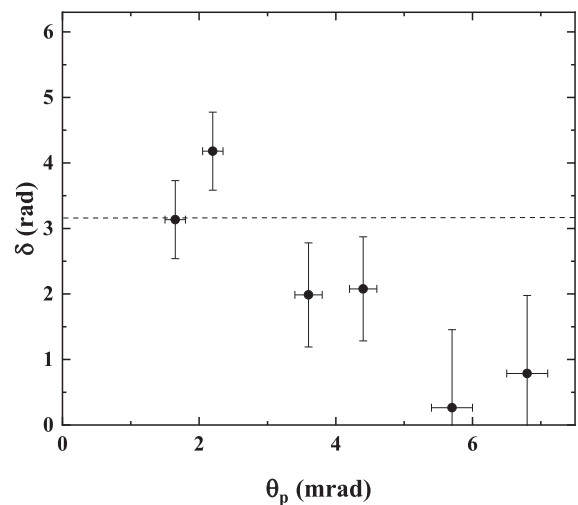


FIG. 4. Phase-shift  $\delta$  in the interference term extracted from the location of the interference extrema under the assumption that the transition always occurs at the classical inner turning point of the initial vibrational state ( $D = 1.2$  a.u.).

It is not unreasonable to assume that for the perpendicular orientation  $\delta$  depends on  $\theta_p$  as well (although one would not necessarily expect the same dependence as for the parallel orientation). If that is the case then even for this orientation, despite the constant  $\mathbf{q}_{tr} \cdot \mathbf{D}$ , an interference structure would be expected. However, the oscillation length would probably be considerably longer than for the parallel orientation. For example, the period of oscillation for the parallel orientation due to  $\delta(\theta_p)$  alone (i.e., ignoring  $\mathbf{q}_{tr} \cdot \mathbf{D}$ ) would be about 8 mrad according to Fig. 4. An oscillation with such a long period, superimposed on steeply decreasing incoherent cross sections, may be difficult to identify, especially at large  $\theta_p$ , where the statistical errors are relatively large. Nevertheless, Fig. 1 shows that the cross sections for the perpendicular orientations significantly drop below those for the parallel orientation between  $\theta_p = 1.5$  and 5 mrad and the two data sets then approach each other again at very large  $\theta_p$ . This might be a signature of a large-period interference oscillation.

The solid lines in Fig. 2 show our theoretical calculations based on a distorted wave approach. The details of this model were published previously [16,17]. In short, the transition amplitude is obtained within an impact parameter formulation and includes the interaction between the projectile and each nucleus of the molecule  $V_{nm}$ . Vibrational dissociation is accounted for by convoluting the spatial part of the transition amplitude with the overlap between the initial and final vibrational states. The  $\theta_p$ -dependent transition amplitude is then obtained as a Fourier transform of the impact parameter-dependent amplitude. As in the experimental data, the FDCS were integrated over KER from 0 to 2 eV.

As in the experimental data, the calculation, too, exhibits a pronounced oscillatory structure with minima at 1.07, 2.9, 4.6, and 6.1 mrad and maxima at 1.8, 3.7, and 5.3 mrad. Thus, the oscillation length, ranging between 1.5 and 1.9 mrad, depending on  $\theta_p$ , is somewhat smaller than in the experimental data (1.9–2.3 mrad). However, the location of the interference extrema is quite sensitive to the oscillation length and this leads to significant discrepancies between theory and experiment. Furthermore, the  $\theta_p$  dependence of the theoretical cross sections is much steeper compared to the measured cross sections. This could be indicative for an underestimation of the importance of  $V_{nm}$ , which is expected to have a particularly large effect at large  $\theta_p$ .

The discussion of the FDCS integrated over KER = 0 to 2 eV strongly suggests that the phase-shift  $\delta$  depends on  $\theta_p$ . In the following we will investigate whether  $\delta$  also depends on the KER. To this end, the FDCS for the parallel orientation are plotted for fixed KER, as indicated in the insets, as a function of  $\theta_p$  in Fig. 5. Interference extrema are observed at about the same  $\theta_p$  as in the FDCS integrated over KER, although at large  $\theta_p$  the lower statistics makes an accurate determination of the location of the extrema difficult. Furthermore, we cannot identify any difference in the location of the extrema between the FDCS for the various KER. This shows that  $\delta$  has a much weaker, if any, dependence on KER than on  $\theta_p$ . Contrary to the experimental data, the calculation (solid lines in Fig. 5) shows a significant dependence of the location of the interference extrema on KER. In Fig. 6 the calculations for the various KER are compared and it can be seen that with increasing KER the interference extrema systematically move to larger

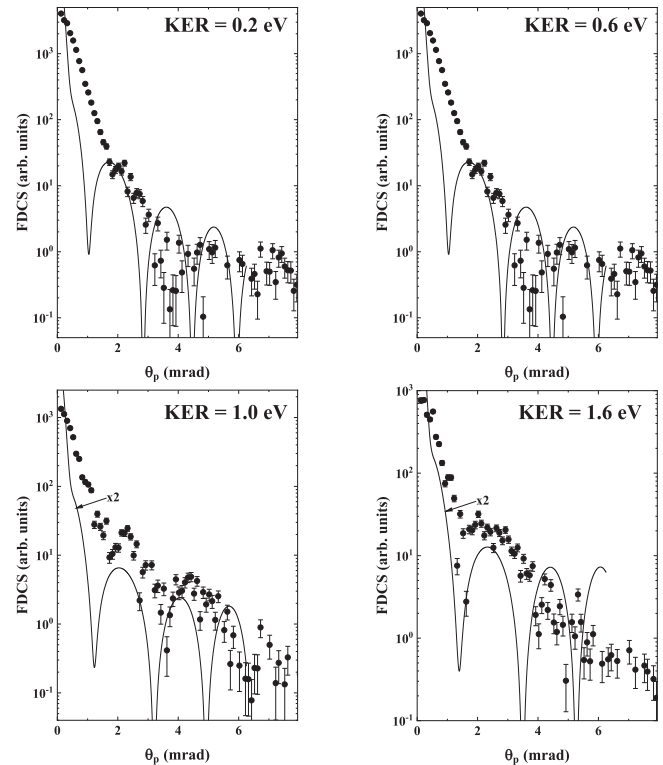


FIG. 5. Fully differential cross sections for the parallel molecular orientation for various fixed values of KER (see insets) as a function of projectile scattering angle. The solid lines show our calculations.

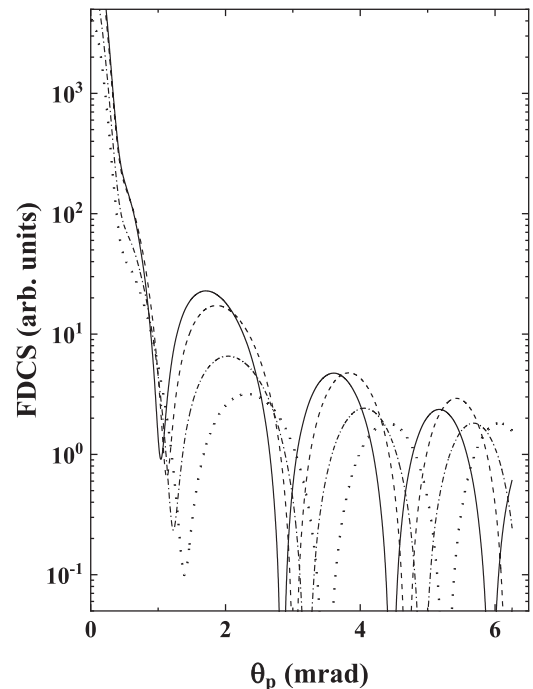


FIG. 6. Comparison of the theoretical fully differential cross sections for the KER values of Fig. 5 to illustrate the dependence of the location of the interference extrema on the KER. Solid curve, KER = 0.2 eV; dashed curve, KER = 0.6 eV; dashed-dotted curve, KER = 1.0 eV; dotted curve, KER = 1.6 eV.

$\theta_p$ . As a result, the agreement between experiment and theory tends to be somewhat better at large KER than at small KER.

The experimental observations and the comparison to theory raise several questions:

(a) Why is the interference term afflicted with a nonzero phase shift although the molecular transition does not involve a change of symmetry?

(b) Why does the phase shift depend on  $\theta_p$ , but not on KER?

(c) Why is the interference structure not visible for  $\theta_p < 1.5$  mrad?

(d) Why are the dependencies of the interference term on  $\theta_p$  and KER so different between experiment and theory?

In the following we will offer a hypothetical explanation addressing these questions, for which, however, we cannot yet provide conclusive evidence. It is based on a classical analogy. It is well known that mechanical waves reflected from a fixed end suffer a phase leap of  $\pi$ . The quantum-mechanical equivalent is reflection of a particle wave from a potential wall of infinite height. Such a scenario is approximately realized in nuclear excitation to a vibrational continuum state. Although the potential does not step up sharply at a well-defined location to infinity, as for a potential wall, the potential-energy curves of the molecular states do rise very steeply as  $D$  decreases and asymptotically go to infinity. Therefore, if the vibrational wave packet propagates towards decreasing  $D$  immediately after the transition, one would expect a reflection of the wave packet near the inner turning point with a  $\pi$ -phase leap resulting in dissociation as the reflected wave packet propagates towards increasing  $D$ .

While reflection of the vibrational wave packet preceding dissociation is generally possible, it obviously is not a prerequisite for dissociation. In a direct path, where the wave packet immediately propagates towards increasing  $D$ , no reflection occurs, and one would consequently not expect any phase leap. In the experiment, it cannot be distinguished whether dissociation proceeds through the direct or the reflection path and each may occur with some probability. The cross sections would then reflect a combination of the interference terms with and without  $\pi$ -phase shift. Equal probabilities would then result in a vanishing interference term. Likewise, an interference structure with phase shift would be indicative of a dominant reflection path and one without phase shift would be indicative of a dominant direct path.

Based on these arguments the data of Fig. 4 suggest that the reflection path is favored at small  $\theta_p$  (but not smaller than 1.5 mrad) and the direct path at large  $\theta_p$ . This dependence of  $\delta$  on  $\theta_p$  can be understood within a classical picture. If the impact parameter  $b$  (relative to the center of mass of the molecule) is smaller than  $D/2$  at the instance of the transition, then the projectile will exert a repulsive force on both protons of the molecule driving them apart (corresponding to the direct path). If, on the other hand  $b$  is larger than  $D/2$ , both molecular protons are repelled in the same direction by the projectile. However, the strength of the force will be larger on the proton which is closer to the projectile, resulting in a tidal force which will push the two protons closer together (corresponding to the reflection path). Since small  $b$  are more selective on large  $\theta_p$  and large  $b$  on small  $\theta_p$  this

could explain the dependence of  $\delta$  on  $\theta_p$  observed in Fig. 4. The magnitude of the tidal force maximizes at  $b = D/2$  and goes asymptotically to zero for  $b$  approaching infinity. Therefore, for very small  $\theta_p$  the effect of the tidal force pushing both protons closer together becomes negligible. In this case, the interaction of the projectile with the molecular protons merely displaces the center of mass of the molecule, but it does not significantly affect the relative motion between the two protons. This scenario favors neither the direct nor the reflection path, which would explain the vanishing of the interference structure observed in the experimental data for  $\theta_p < 1.5$  mrad.

The observation that the phase shift does not depend on the KER is not surprising. In contrast to dissociation through electronic excitation, in vibrational dissociation there is not a strong correlation between the KER and  $D$ . All vibrational continuum states are accessible in the entire Franck-Condon region of the ground state of  $H_2$ . At the same time, the total energy of the molecule is constant for each vibrational state, i.e., it does not depend on  $D$  within the Franck-Condon region. Therefore, one would expect  $D$  corresponding to the inner turning point to be favored regardless of the KER due to the maximized overlap between the initial and final vibrational-state wave functions. However, the observed independence of the location of the interference extrema on the KER appears to be in conflict with our calculations, in which we find a significant dependence on the KER. At present, we do not have an explanation for this difference between the experimental data and the calculations and further studies are called for.

## V. CONCLUSIONS

We have presented a joint experimental and theoretical study on vibrational dissociation following electron capture in 75-keV  $p + H_2$  collisions. The complete kinematic information of all collision fragments in the final state was determined, from which fully differential cross sections FDCS were extracted. Our analysis focuses on a molecular orientation perpendicular to the initial projectile beam axis and parallel to the transverse momentum transfer. A pronounced two-center molecular interference structure was observed in both the experimental data and in the calculated FDCS as a function of projectile scattering angle  $\theta_p$ . However, there are significant discrepancies between the measured and calculated data.

Previously we reported on data for the same process and the same kinematics but integrated over the entire KER region in which vibrational dissociation can occur [10]. There, we found a phase shift which was thought to be constant at  $\pi$  for all  $\theta_p$ . A more detailed analysis of the new data suggests that the phase shift actually varies between  $\pi$  at relatively small  $\theta_p$  and nearly 0 at large  $\theta_p$ . The FDCS for fixed KER exhibit interference extrema at about the same locations as in the cross sections integrated over KER. This suggests that the phase shift is (nearly) independent of the KER. In contrast, in our calculations the locations of the interference extrema significantly depend on the KER.

We have presented a hypothetical explanation for these observations. It assumes that the vibrational wave packet can

either propagate towards larger internuclear distances, which results in direct dissociation because the molecule is in a vibrational continuum state, or towards smaller internuclear distances. In this case the wave packet has to be reflected at the inner turning point before dissociation can occur. Such a reflection from a steep potential wall results in a phase leap manifesting itself in a corresponding phase shift in the interference term. Within a classical picture we argued that relatively small (but not too small)  $\theta_p$  should favor the reflection path and large  $\theta_p$  the direct path. Within our model both paths should occur with similar probabilities for very small  $\theta_p$ . This would explain the vanishing of the interference structures at these very small scattering angles. However, we emphasize that we do not claim ultimate evidence for the correctness of our model. Rather, we hope that it will trigger

further theoretical studies to either confirm or dismiss our explanation for the phase shift.

We further emphasize that if our model is confirmed the explanation for the phase shift is qualitatively different from the reason for a similar (but constant) phase shift observed in dissociation following electronic excitation to an antisymmetric dissociative state, where the explanation is based on parity conservation [5].

#### ACKNOWLEDGMENTS

This work was supported by the National Science Foundation under Grant No. PHY-2011307. Valuable discussions with Dr. Raul Barrachina and Dr. Marcelo Ciappina are gratefully acknowledged.

- 
- [1] T. F. Tuan and E. Gerjuoy, *Phys. Rev.* **117**, 756 (1960).  
 [2] S. Cheng, C. L. Cocke, V. Frohne, E. Y. Kamber, J. H. McGuire, and Y. Wang, *Phys. Rev. A* **47**, 3923 (1993).  
 [3] N. Stolterfoht, B. Sulik, V. Hoffmann, B. Skogvall, J. Y. Chesnel, J. Rangama, F. Frémont, D. Hennecart, A. Cassimi, X. Husson, A. L. Landers, J. A. Tanis, M. E. Galassi, and R. D. Rivarola, *Phys. Rev. Lett.* **87**, 023201 (2001).  
 [4] D. Misra, U. Kadhane, Y. P. Singh, L. C. Tribedi, P. D. Fainstein, and P. Richard, *Phys. Rev. Lett.* **92**, 153201 (2004).  
 [5] L. Ph. H. Schmidt, S. Schössler, F. Afaneh, M. Schöffler, K. E. Stiebing, H. Schmidt-Böcking, and R. Dörner, *Phys. Rev. Lett.* **101**, 173202 (2008).  
 [6] H. T. Schmidt, D. Fischer, Z. Berenyi, C. L. Cocke, M. Gudmundsson, N. Haag, H. A. B. Johansson, A. Källberg, S. B. Levin, P. Reinhard, U. Sassenberg, R. Schuch, A. Simonsson, K. Stöckel, and H. Cederquist, *Phys. Rev. Lett.* **101**, 083201 (2008).  
 [7] J. S. Alexander, A. C. Laforge, A. Hasan, Z. S. Machavariani, M. F. Ciappina, R. D. Rivarola, D. H. Madison, and M. Schulz, *Phys. Rev. A* **78**, 060701(R) (2008).  
 [8] L. Ph. H. Schmidt, T. Jahnke, A. Czasch, M. Schöffler, H. Schmidt-Böcking, and R. Dörner, *Phys. Rev. Lett.* **108**, 073202 (2012).  
 [9] S. F. Zhang, D. Fischer, M. Schulz, A. B. Voitkiv, A. Senftleben, A. Dorn, J. Ullrich, X. Ma, and R. Moshhammer, *Phys. Rev. Lett.* **112**, 023201 (2014).  
 [10] B. R. Lamichhane, T. Arthanayaka, J. Remolina, A. Hasan, M. F. Ciappina, F. Navarrete, R. O. Barrachina, R. A. Lomsadze, and M. Schulz, *Phys. Rev. Lett.* **119**, 083402 (2017).  
 [11] A. Messiah, in *Quantum Mechanics* (North-Holland, Amsterdam, 1970), Vol. II, pp. 848–852.  
 [12] B. R. Lamichhane, A. Hasan, T. Arthanayaka, M. Dhital, K. Koirala, T. Voss, R. A. Lomsadze, and M. Schulz, *Phys. Rev. A* **96**, 042708 (2017).  
 [13] A. Senftleben, T. Pflüger, X. Ren, O. Al-Hagan, B. Najjari, D. Madison, A. Dorn, and J. Ullrich, *J. Phys. B* **43**, 081002 (2010).  
 [14] R. Barrachina, private communication (2019).  
 [15] M. F. Ciappina, O. A. Fojon, and R. D. Rivarola, *J. Phys. B* **47**, 042001 (2014).  
 [16] A. Igarashi and L. Gulyas, *J. Phys. B* **52**, 075204 (2019).  
 [17] A. Igarashi, *J. Phys. B* **53**, 225205 (2020).  
 [18] K. N. Egodapitiya, S. Sharma, A. Hasan, A. C. Laforge, D. H. Madison, R. Moshhammer, and M. Schulz, *Phys. Rev. Lett.* **106**, 153202 (2011).  
 [19] W. C. Wiley and I. H. McLaren, *Rev. Sci. Instrum.* **26**, 1150 (1955).  
 [20] T. P. Arthanayaka, S. Sharma, B. R. Lamichhane, A. Hasan, J. Remolina, S. Gurung, and M. Schulz, *J. Phys. B* **48**, 071001 (2015).  
 [21] T. E. Sharp, *Atomic Data* **2**, 119 (1971).  
 [22] A. Senftleben, T. Pflüger, X. Ren, B. Najjari, A. Dorn, and J. Ullrich, *J. Phys. B* **45**, 021001 (2012).